Skeletal Radiology (2022) 51:1787–1796
https://doi.org/10.1007/s00256-022-04020-w

SCIENTIFIC ARTICLE

Update on MRI findings of osteomyelitis of long bones in the adult population

Julia Crim[1] · Samantha Salmon[1] · Christy Waranch[1] · Jacob Elfrink[1] · Eleanor Layfield[2] · J. Derek Stensby[1]

Received: 28 September 2021 / Revised: 15 February 2022 / Accepted: 15 February 2022 / Published online: 28 February 2022

Abstract

Objectives To evaluate the usefulness of new and established MRI signs of osteomyelitis in long bones in adults.

Methods All patient records over a 9-year period with clinical or MRI suspicion for osteomyelitis were retrospectively reviewed, using strict criteria for proof of infection. Two musculoskeletal radiologists independently reviewed the MRIs of proven osteomyelitis.

Results Out of 45 MRIs of confirmed osteomyelitis, 2 MRIs (4%) did not show confluent low-signal intensity on T1-weighted images, but all showed confluent high-signal intensity on T2-weighted images. Central hypoenhancing regions of marrow without abscess formation were found in 15–18/35 (43–51%) cases where gadolinium was given. We often found multiple foci of marrow replacement in the same bone. The areas of marrow involvement often had an irregular contour. Penumbra sign, marrow fat globules, and sequestra were uncommon.

Conclusion Multiple foci of bone marrow signal abnormalities, an irregular contour of marrow abnormality, and central marrow hypoenhancement without abscess are common signs of osteomyelitis of long bones in adults. Confluent low T1-signal intensity is not always present.

Keywords Osteomyelitis · Hematogenous osteomyelitis · Pressure ulcer · Bone infarct · MRI of osteomyelitis

Abbreviations

OM	Osteomyelitis
HOM	Hematogenous osteomyelitis
COM	Osteomyelitis due to contiguous spread
ESR	Erythrocyte sedimentation rate
CRP	C-reactive protein
MRI	Magnetic resonance imaging

Key points

1. A small number of cases of proven osteomyelitis lack confluent low signal intensity on T1-weighted images, while all show confluent high signal on T2-weighted images.
2. Osteomyelitis, especially when due to hematogenous spread, often shows a pattern of multiple separate areas of marrow abnormality.
3. Osteomyelitis often shows central contrast hypoenhancement without abscess formation and its irregular contour may mimic a bone infarct.
4. Previously described findings of marrow fat globules, subperiosteal abscess, penumbra sign and intraosseous abscess were uncommon in our patient population.

Introduction

Radiographs are the initial imaging modality for osteomyelitis (OM) because they are safe, accessible, and cost-effective [1]. However, they may be false negative for OM, and magnetic resonance imaging (MRI) is an important tool in the clinical diagnosis of OM [2].

✉ Julia Crim
crimj@health.missouri.edu

Samantha Salmon
Sld748@health.missouri.edu

Christy Waranch
waranchcm@health.missouri.edu

Jacob Elfrink
elfrinkj@health.missouri.edu

Eleanor Layfield
Eleanorlayfield95@gmail.com

J. Derek Stensby
stensbyj@health.missouri.edu

[1] University of Missouri at Columbia, 1 Hospital Dr, Columbia, MO 65212, USA

[2] University of Pennsylvania, Philadelphia, PA, USA

The reported sensitivity of MRI for OM varies in different patient populations and with different techniques but is high [1, 3, 4]. Reported MRI findings in adult patients include confluent low T1/high T2 signal intensity in the marrow, cortical breakthrough, and periosteal reaction.

The initial descriptions of the MRI appearance of OM date from the early years of MRI, when spatial resolution and sequences were limited [5, 6]. Subsequent studies of MR findings of OM have focused on the problem of pedal osteomyelitis in diabetic patients. Diabetic pedal OM is due to direct spread from soft-tissue ulcers. MRI findings include cortical breakthrough and an underlying, confluent focus of low T1, high T2 signal marrow replacement with rounded margins [7, 8]. To our knowledge, the reports of MRI findings of long bone OM in adults are anecdotal [1, 9–12]. There is good data on findings in the pediatric population. However, the children have a very different blood supply and periosteal composition than adults, and as a result, the MRI appearance of pediatric OM is different from what is found in adults [13–16]. Howe and colleagues performed a retrospective review of T1-weighted signal characteristics in histopathologically proven, nonpedal OM in a population which included both adults and children [12]. They found that among 21 cases of HOM, there were 4 where the T1-weighted imaging features were atypical: 2 with subcortical, hazy, reticulated decreased T1 signal and 2 with T1 signal that was not decreased relative to skeletal muscle.

This retrospective observational study was undertaken in order to investigate how the findings of adult nonpedal osteomyelitis compare to those of pedal osteomyelitis.

Methods

Patient selection

The study was IRB-approved and HIPAA compliant. MRI reports of patients 18 years of age or older were searched from January 2011 to Dec 2020 for the word "osteomyelitis." There were 3916 cases meeting that basic criterion. Cases were excluded if no osteomyelitis was diagnosed, or if the abnormalities did not involve the long bones. The reports for all cases where osteomyelitis was included in the differential diagnosis on MRI in the long bones were then reviewed. MR images and other medical records were reviewed as needed, allowing us to classify cases as suspicious for hematogenous spread (HOM) or contiguous spread (COM). Postoperative osteomyelitis and cases where the source of infection was unclear were excluded. Pathology records for the same time period were independently reviewed using the same criteria, in order to identify any cases where pathology was positive but MRI was negative.

A chart search was then performed in the cases we identified, to determine if they met the current clinical diagnostic criteria of OM, shown in Tables 1 and 2 [17–19]. Erythrocyte sedimentation rate (ESR) and C-reactive protein (CRP) were not used as diagnostic criteria in our series, because both ESR and CRP may yield false-positive and false-negative results and because there is a wide variance in the threshold values considered to be suspicious for OM [20–22].

Figure 1 shows the decision tree used to identify patients for the purposes of the study. Ten cases that included HOM in the original MRI differential diagnosis were excluded because of different final diagnoses: 2 cases of bone infarcts, 1 case of marrow changes related to end-stage renal disease (confirmed on bone biopsy), 1 case of metastatic disease, 1 case of radiation necrosis, 1 case of grade 2 chondrosarcoma, 1 case of sickle cell disease without defined infarct but no infection on clinical follow-up, 2 cases of normal erythropoietic marrow (perception error by initial interpreting radiologist), and 1 case where the only surgical pathology diagnosis was osteoarthritis.

When patients presented with suspected COM from amputation, wound, or pressure ulcer, rigorous proof of infection was often lacking in the patient record, and many cases suspicious for OM were not eligible for our study for that reason. Of 31 suspected cases where documentation

Table 1 Criteria for diagnosis or exclusion of hematogenous osteomyelitis

Positive for HOM
1. No history of surgery or penetrating injury to the area, no adjacent amputation, no inflammatory arthritis, and no soft tissue wound AND
2. Confluent marrow replacement on MRI seen on T1 or fluid-sensitive sequences AND
3. One or more of the following criteria:
a. Bone or periosteal or joint fluid culture positive for elevated WBC in absence of inflammatory arthritis, whether or not bacterial growth was seen on culture
b. Positive blood culture
c. Osteomyelitis diagnosed on surgical pathology
Negative for HOM
Marrow replacement on MRI where another cause of abnormality was documented, or clinical follow up > 1 year without treatment did not show evidence of infection

Table 2 Criteria for diagnosis or exclusion of osteomyelitis by contiguous spread

Positive for COM
1. Sinus tract or wound extending to bone AND
2. Confluent marrow replacement on MRI seen on T1 or fluid-sensitive sequences plus one or more of the following:
a. Positive local culture or histology
d. Purulent material found at time of surgery
Negative for COM
1. Negative histology plus follow-up for > 1 year without evidence of infection OR
2. Clinical findings and laboratory values did not indicate osteomyelitis OR
3. Other cause of marrow abnormality found

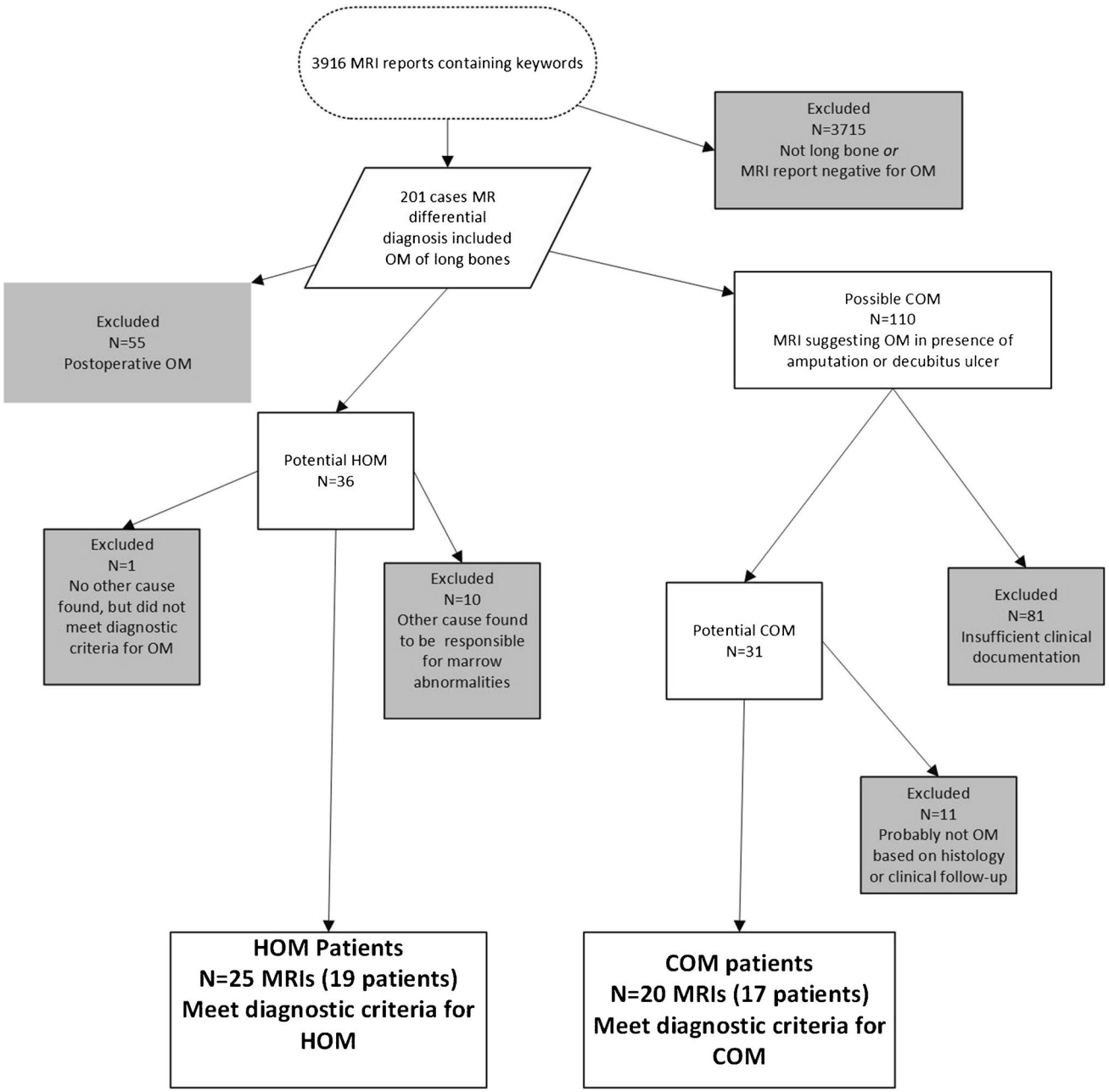

Fig. 1 Decision tree for evaluation of possible cases of OM on MRI. HOM, hematogenous osteomyelitis; COM, osteomyelitis by contiguous spread

met our criteria, 11 were excluded: 4 definitively not OM based on negative biopsy plus follow-up of 2 or more years, and 7 probably not infected based on clinical findings and follow-up of 1 year or more. Two patients with COM had 2 consecutive MRIs, which were analyzed separately. Two patients had MRIs showing documented COM of both lower extremities.

MRI evaluation

The MRIs which met the criteria for OM were retrospectively and independently reviewed by 2 MSK radiologists (1 with 7 years and 1 with 30 years of experience) for the following published signs of osteomyelitis: confluent marrow replacement which was low T1 and/or high T2 signal intensity, cortical breakthrough, periosteal reaction including subperiosteal abscess, fat globules in the medullary space [23], intraosseous gas, the penumbra sign [24], marrow enhancement after administration of intravenous gadolinium, and intraosseous abscess (Brodie abscess). Hypoenhancing regions of marrow within a focus of osteomyelitis, without the peripheral rim of enhancement seen in an abscess, have been reported in children [13] but not in adults. We assessed all cases for this finding. We noted when reticulated marrow edema, defined as feathery, nonconfluent low T1 and high T2 signal, was present. Additionally, cases were evaluated for 2 previously unpublished signs of OM which we had observed clinically. The first of these is an irregular contour as opposed to the usual rounded contour of neoplasms. The second sign is the presence of multiple separate foci of confluent marrow abnormality.

All cases were evaluated for signs of septic arthritis and soft tissue infection. Septic arthritis was diagnosed when joint effusion, irregularly thickened synovium, and marrow abnormalities of the opposite side of the joint were present, with or without bone erosions.

MRIs were performed on Siemens Skyra and Aera systems and GE Signa Magnetom, Artist, and Architect systems, using dedicated surface coils. All patients had T1-weighted and fluid-sensitive sequences in at least 2 planes. Gadolinium was administered in 20/25 (80%) HOM cases and 15/20 (75%) COM cases.

Statistical analysis

STAT-X 9 software was used. Agreement between 2 observers was done utilizing AC1, which is widely utilized in preference to kappa in correcting for chance agreement [25]. Comparison of frequency of signs of OM between HOM and COM was computed using Fisher's exact test, which is preferable to chi-squared for small data sets.

Table 3 Characteristics of OM patients

Characteristic	HOM	COM
Unique patients	19	18
Number of MRIs	25	20
age	18–88 (mean 48)	22–79 (mean 49)
gender	11 male, 8 female	11 male, 7 female
Underlying predisposing disease or event*	11/19 (53%)	18/18
Prior closed trauma	4/19 (21%)	0
ESR**	12–130 (mean 77)	43–130 (mean 92)
CRP***	0.9–70 (mean 11)	0.4–18.6 (mean 8)
Center of infection	Diaphysis 10/22 (45%)**** Metaphysis 4/22 (18%) Epiphysis/apophysis 8/22 (36%)	Adjacent to ST infection in all cases
Symptom duration prior to MRI	Unknown for 10 MRI's 14–240 days (mean 81 days, in 15/25 MRI's where onset known)	unknown

* HOM underlying conditions: intravenous drug use (4), diabetes mellitus (3), splenectomy (1), concurrent deep venous thrombosis (1), treated lymphoma (2), prior lumbar puncture (1)

COM underlying conditions: paraplegia with chronic pressure ulcers (5), traumatic leg wound (1), amputations performed for diabetes or trauma (12)

** normal ESR value in our laboratory < 30 mm/h

*** normal CRP value in our laboratory < 0.5

**** note that 3 patients with HOM had 2 contiguous bones involved

Results

Patient cohort

Clinical and laboratory characteristics of the 2 groups of patients are listed in Table 3.

HOM patients

There were 19 unique patients in whom a diagnosis of HOM of long bones could be confidently made based on the criteria listed in Table 1. Three patients had 2 MRIs, performed at different time points during the course of the infection. Three patients had bilateral HOM. This made a total of 25 MRI studies of HOM. Causative organisms were identified in 15 cases. These were *Staphylococcus aureus* (9), streptococcal species (2), fusobacteria (1), *Serratia* species (1), an unspecified bacillus (1), and *Escherichia coli* in association with *Candida albicans* (1).

COM patients

COM of long bones could be confidently diagnosed based on the criteria listed in Table 2 in 20 MRIs (18 patients).

Causative organisms were identified in 14 cases: Enterococcus (5), *Staphylococcus aureus* (3), polymicrobial (5), group B beta-hemolytic streptococcus (1).

MRI findings.

The MRI findings in our cohort are summarized in Table 4. It is evident that there are both commonalities and differences in the appearance of HOM (Figs. 2 and 3) and COM (Figs. 4 and 5) of the long bones. Differences between HOM and COM reached statistical significance ($p < .05$) for hypoenhancing marrow, more common in HOM, absence of confluent T1 signal, seen in DOM only, presence of multiple foci, which were more common in HOM, and septic arthritis, seen almost exclusively in HOM.

Both HOM and COM showed confluent high signal intensity marrow replacement on fluid-sensitive sequences. However, 2 cases of COM did not show definite confluent low-signal intensity T1 weighted marrow replacement. There was a contrast enhancement of OM in all cases where it was administered. Reticulated marrow abnormalities surrounded the confluent abnormalities in the majority of cases. The periosteal reaction was visible in the majority of both types of osteomyelitis. Several previously reported signs were uncommon in both types of

Table 4 MRI findings of HOM and COM

Sign	HOM	COM	Interobserver consistency
Confluent low T1	25/25 (100%)	18/20 (90%)	1.0
Confluent high T2	25/25 (100%)	20/20 (100%)	1.0
Multiple foci	16–18/25 (64–72%)	2–3/20 (1–2%)	.81
Reticulated marrow edema	23–25/25 (92–100%)	17/20 (85%)	.74
irregular contour	14/25 (56%)	8/20 (40%)	1.0
Penumbra sign	5–6/25 (20–24%)	0–2/20 (0–10%)	.68
Marrow enhancement	20/20 (100%)	15/15 (100%)	1.0
Hypoenhancing marrow	15–18/20 (75–90%)	3/15 (20%)	.64
Fat globules	3/25 (8%)	0/20 (0%)	1.0
Sequestrum	1/25 (4%)	1/20 (5%)	1.0
Cortical breakthrough	22/25 (88%)	20/20 (100%)	1.0
Periosteal reaction	22–25/25 (88–100%)	19–20/20 (95–100%)	.87
Joint effusion	19/25 (76%)	5/20[1] (25%)	1.0
Septic arthritis	17/25	1/20[1] (5%)	1.0
Sinus tract from bone to skin	0/25 (0%)	18/20 (90%)	1.0
Wound abutting bone	0/25 (0%)	2/20 (10%)	1.0
Soft tissue abscess	8/25 (32%)	1/20 (5%)	1.0

Note: Ranges of case numbers describes the assessment of 2 different observers

Some patients had more than one MRI; findings of each MRI are reported separately

[1]Seen only in cases of pressure ulcer of the proximal femur

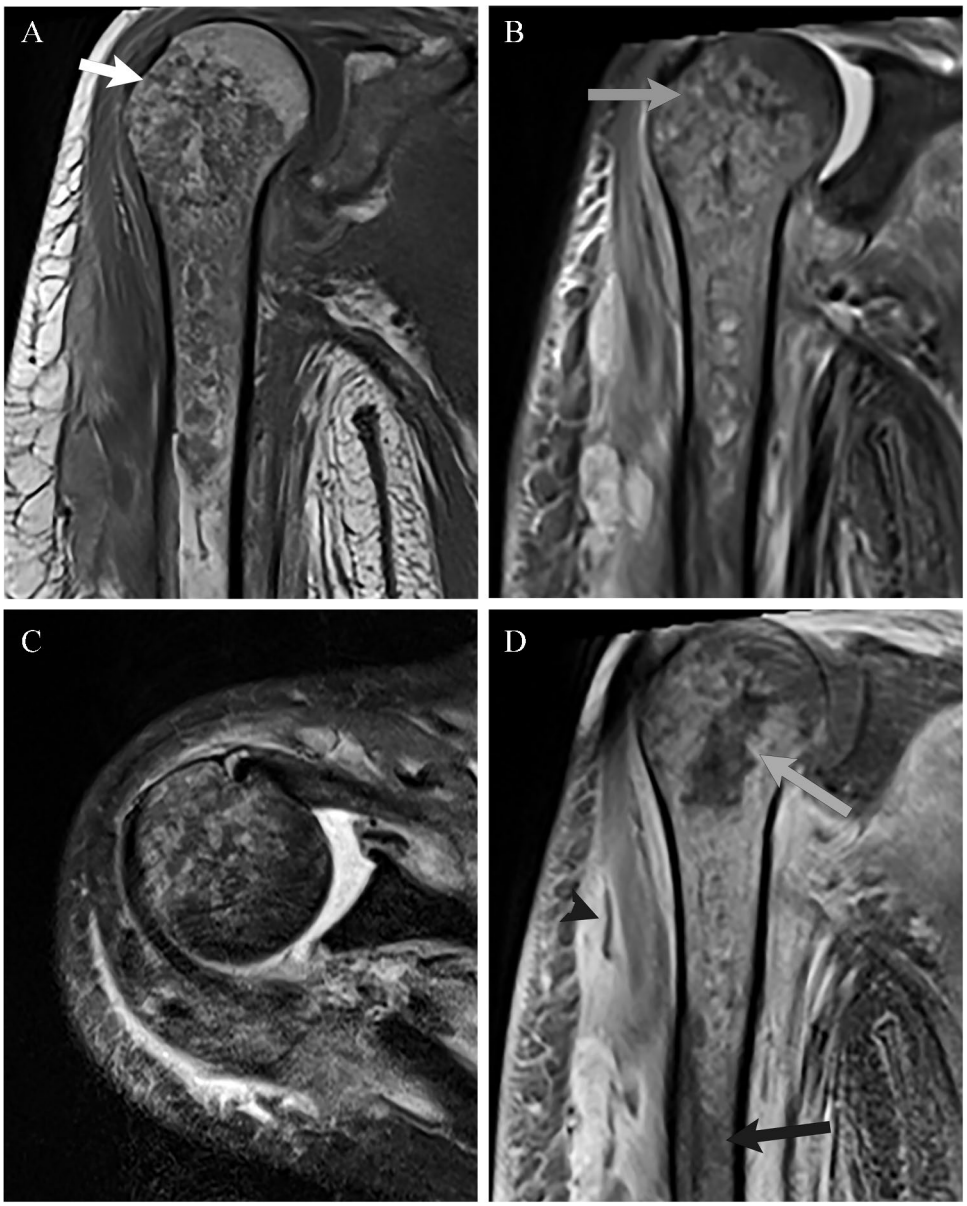

Fig. 2 A twenty-five-year-old woman with a history of intravenous drug use and endocarditis, MRI showing osteomyelitis. **A** Coronal T1WI (TR 608/TE 8.8) at 3 T (Siemens Skyra) shows multiple foci of low signal intensity separated by normal marrow fat. At the periphery of the abnormal regions are small foci of abnormal marrow (arrow). Multiple larger, confluent areas have an aggregate irregular contour. Areas of reticulated edema are present peripheral to the more confluent regions. **B** Coronal STIR (TR 4800/TE 22/TI 200) shows small areas of abnormally high signal intensity marrow in the proximal metaphysis (arrow), as well as larger areas of irregularly shaped, confluent abnormal high signal intensity in the marrow. Fluid collections are seen in the surrounding muscles. **C** Axial T2FS (TR 3300/TE75) shows multifocal areas of high signal intensity corresponding to the areas of abnormality on the T1-weighted image. **D** Coronal T1WFS post gadolinium image (TR733/TE 8.8) shows that both the small areas and the majority of the larger areas of abnormal marrow enhance. However, there is a central non-enhancing region (gray arrow), which is lower signal intensity than normal humeral marrow distal to the infection (black arrow). There are small abscesses in the surrounding muscles, one shown by arrowhead

OM in our series: the penumbra sign, intramedullary fat globules, and sequestra.

HOM and COM showed a somewhat different pattern of marrow involvement. The majority of cases of COM showed a single focus of marrow replacement adjacent to a cortical defect, while HOM typically showed multiple distinct foci, often very small, of abnormal marrow, and an irregular contour. Both HOM and COM often had an irregular contour. Central hypoenhancing areas were seen much more commonly in HOM than in COM.

OM over time

Three cases of HOM underwent serial MRIs. The findings of the patient shown in Fig. 3 were mistaken for bone infarct on the initial MRI, and the patient was not treated for an infection until after the 2nd MRI. This case provides an example of the evolution of MRI findings in early untreated HOM.

Discussion

Osteomyelitis (OM) may occur due to several different routes of pathogen spread: contiguous spread from an adjacent infected soft tissue wound (COM), penetrating trauma, contamination at the time of surgery, or hematogenous spread (HOM)[26].

COM is by far the most common type of OM in adults. It is a frequent infection deep to diabetic foot ulcers and also

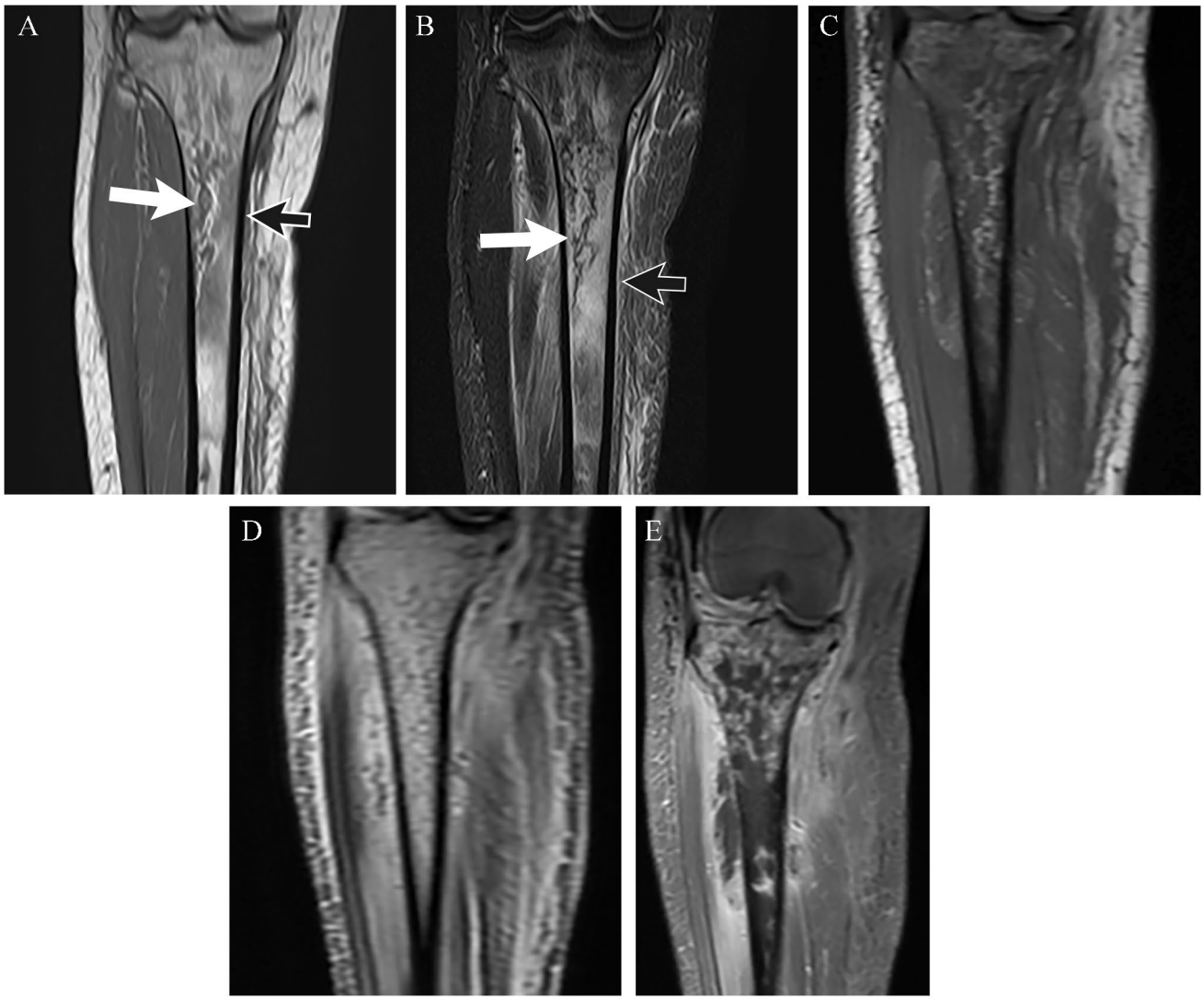

Fig. 3 Physically active 18-year-old woman presenting with 14-day history of malaise and leg pain. An MRI was obtained at the time of presentation (**A**, **B**). The original radiologist's interpretation was bone infarct, and the patient was treated with analgesics only. Her symptoms worsened, and the MRI was repeated 2 weeks later (**C**–**E**). Blood culture and biopsy yielded MRSA. **A** T1-weighted coronal image shows multiple areas of low signal intensity marrow, with interposed fat. Several of the abnormal areas show a serpentine contour (white arrow), while others do not (black arrow). Peripheral areas of reticulated marrow surround the more confluent regions. **B** Coronal STIR image shows high signal intensity corresponding to the low signal regions on T1 weighted image. Periosteal reaction, also found in bone infarcts, is present (black arrow). **C** T1-weighted coronal image 14 days after A and B shows that the multiple areas of low-signal marrow have progressed, while still showing interspersed fat between the foci. **D** Coronal STIR image shows corresponding high signal intensity marrow abnormalities and progressive soft tissue abnormalities. **E** Coronal T1-weighted fat-suppressed post gadolinium image shows that there are multiple areas of marrow that are hypoenhancing compared to normal marrow in the distal femur. A discrete intraosseous abscess has not formed, however. There is an abscess in the anterior compartment muscles

occurs adjacent to amputations, pressure ulcers, and deep soft tissue wounds. Eighty-five percent of cases of HOM arise in children, most commonly involving the metaphysis of long bones [17, 27]. In adult patients, HOM most commonly involves the vertebral bodies [15, 28]. The distribution of HOM reflects the vascular supply to the bone [15, 29]. Vascularity depends on patient age, type of bone (long bone vs. flat bone vs. vertebra), and whether or not the patient has had microtrauma to the bone [4, 16, 30, 31].

The significant differences in blood supply between adult and pediatric patients results in different patterns and frequency of HOM. During infancy, long bone metaphyseal and epiphyseal vessels anastomose via the transphyseal vessels, which perforate the growth plate, allowing for diffuse intraosseous infection [13]. Over time, the growth plate forms a barrier between the metaphysis and epiphysis. Adjacent to the growth plate runs a slow-flow, intra-metaphyseal capillary loop. During infection, thrombosis occurs in nutrient

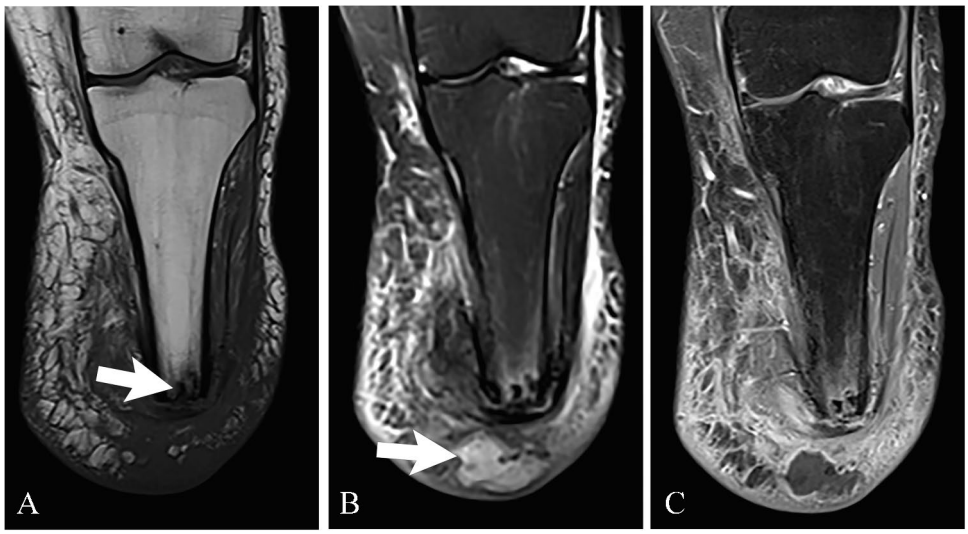

Fig. 4 A 51-year-old man with OM due to staphylococcus aureus after below-knee amputation. He injured the amputation site and developed local erythema and fluctuance. **A** Cor T1WI (TR.TE 606/11) shows small areas of signal void (arrow) at the tip which corresponded to the sclerotic bone on radiographs, and are surrounded by small, irregularly-shaped regions of confluent low T1 signal intensity. **B** Cor T2W FS (TR/TE 4750/75) shows confluent marrow high signal corresponding to low T1 signal areas. Arrow points to soft tissue abscess (arrow). **C** T1WI FS post gadolinium MR shows enhancement around the sclerotic bone. The soft tissue abscess distal to the bone shows peripheral enhancement

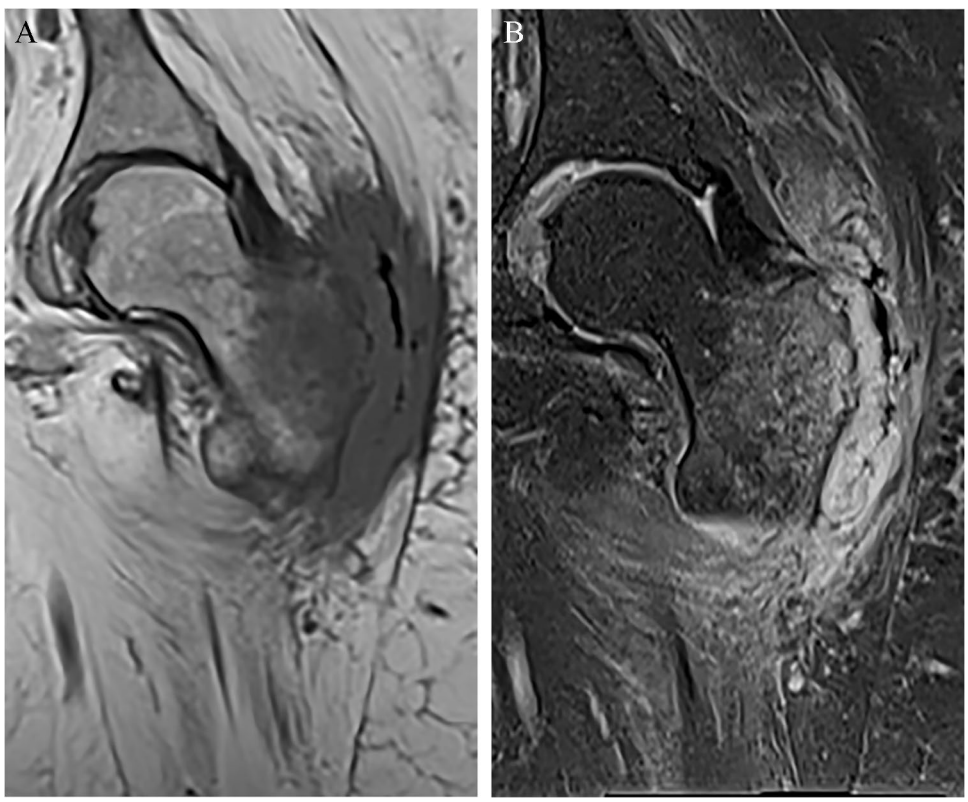

Fig. 5 COM of the proximal femur in a 54-year-old paraplegic woman with deep decubitus ulcer and bone culture positive for OM. **A** Coronal T1WI shows a cortical breakthrough in the femur adjacent to the ulcer. A round, confluent region of low signal intensity is present in the bone marrow as well as small, satellite, low-signal foci. **B** Coronal STIR shows high signal intensity in the central focus and the multiple satellites

arteries from the venous side, causing bacterial stasis and infection contained in the metaphysis [15]. In adulthood, the blood supply to the long bones arrives through diaphyseal, metaphyseal, and epiphyseal blood vessels which generally supply discrete areas of the bone, but may anastomose with each other [16]. Infection in adults also differs from that in children because of changes in the periosteum. During childhood and adolescence, the inner layer of the periosteum (the cambium) is richly vascular and loosely attached to the underlying bone [13]. In contrast, adult cortical blood flow is centrifugal, the periosteum is thin and fibrotic [15], and there are negligible contributions to the medullary cavity from periosteal vessels [16]. For that reason, subperiosteal abscesses are common in cases of pediatric HOM but not in adult cases.

Early detection and diagnosis of OM are important in preventing long-term sequela of bone destruction, deformity, and disability[1]. OM of long bones commonly presents with pain in the affected limb, sometimes accompanied by malaise and low-grade fever [7]. ESR and CRP are typically but not always elevated, and leukocyte count may be normal or only slightly elevated [32, 33]. COM may be polymicrobial, while HOM is almost always from a single pathogenic organism [17, 19, 27, 34]. Similar to a recent large series of cases of bacterial osteomyelitis, we found a variety of causative bacteria, although *Staphylococcus aureus* was the most common [35].

Our study describes the findings of HOM of the long bones in the adult population. There are 3 important findings in our series. First, that confluent low-T1 signal was absent in 2 cases of confirmed OM due to direct spread, although it was present in all cases of HOM. Although confluent T1 abnormal signal has long been a lodestone for diagnosis of OM, it is plausible to presume that there may be a stage of infection where the abnormal marrow signal is not yet confluent. Confluent high T2 signal and enhancement were present in all cases, regardless of the mode of spread of infection.

Second, OM frequently showed multiple foci within a given bone, often very small. We hypothesize that this multifocality may reflect areas of microthrombi and/or increased vascular permeability allowing penetration of bacteria from the vessels. A similar appearance has been described in early bone infarcts [36].

Multifocality is uncommonly seen in primary bone neoplasms and may be useful in suggesting to the interpreting radiologist that OM is more likely than neoplasm.

Third, hypovascular regions and an irregular contour to the marrow abnormalities were both common MRI findings of OM. These findings may mimic bone infarct.

The areas of hypoperfusion seen in OM can be distinguished from intraosseous abscesses because a peripheral ring of enhancement is not present. It may represent vascular compromise caused by infection and could also indicate that pre-existing vascular compromise created an environment in which infection could flourish. Unlike most bone infarcts, the central area of OM showed a low T1/high T2 signal [37]. OM may occur due to superinfection of a bone infarct [38], and we cannot prove that pre-existing infarcts were not present in our patient cohort.

The primary limitation of our study is the small number of patients. This reflects not only the rarity of HOM of long bones in the adult population but also the incomplete documentation of COM adjacent to pressure ulcers in our hospital. Many cases of COM due to pressure ulcers were treated empirically, and documentation of bone infection beyond an abnormal MRI was not performed. Physicians may decide to perform empiric treatment because patients with pressure ulcers are often fragile and chronically ill and maybe receiving chronic antibiotics. Because of the lack of documentation, many cases were excluded which were probably COM. A number of our cases of confirmed COM involved only a small area of bone marrow, as shown in Fig. 4. This may be selection bias, because the treating physicians may have been less likely to obtain confirmatory tests when there was a large area of abnormality on MRI and therefore less doubt in their minds about the diagnosis. Selection bias may also have occurred if OM was present but not included in the differential diagnosis on MRI reports, as shown in Fig. 3. A review of the pathology database at our institution eliminated that potential bias. Interobserver agreement on the presence of diagnostic signs was not perfect, but we believe falls within the expected range of experienced radiologists.

We hope that our newly reported findings of multiple satellite regions of abnormal marrow, central hypoperfusion, and an irregular contour of the marrow abnormalities can increase radiologists' suspicion and level of confidence for the MRI diagnosis of OM. We wish also to emphasize that a confluent low T1 signal is not necessary to make the diagnosis of OM. The previously described findings of fat globules in the marrow, subperiosteal abscess, penumbra sign, and intraosseous abscess were uncommon in our patient population.

It should always be remembered that other entities can have a similar MRI appearance to OM. For this reason, the diagnosis should be confirmed with positive blood cultures, joint aspiration, or bone biopsy.

Acknowledgements The authors thank Lada Micheas, PhD, for her contribution to statistical analysis.

The authors declare no competing interests. Approval from the Institutional Review Board was obtained and in keeping with the policies for a retrospective review, informed consent was not required.

References

1. Tehranzadeh J, Wong E, Wang F, Sadighpour M. Imaging of osteomyelitis in the mature skeleton. Radiol Clin North Am. 2001;39(2):223–50.
2. Beaman FD vHP, Kransdorf MJ, Adler RS, Amini B, Appel M, et al. . ACR Appropriateness Criteria® Suspected Osteomyelitis, Septic Arthritis, or Soft Tissue Infection (Excluding Spine and Diabetic Foot). J Am Coll Radiol [Internet]. https://doi.org/10.1016/j.jacr.2017.02.008: Elsevier Inc; 2017:S326–337.
3. Pineda C, Vargas A, Rodriguez AV. Imaging of osteomyelitis: current concepts. Infect Dis Clin North Am. 2006;20(4):789–825.
4. Lee YJ, Sadigh S, Mankad K, Kapse N, Rajeswaran G. The imaging of osteomyelitis. Quant Imaging Med Surg. 2016;6(2):184–98.
5. Beltran J, Noto AM, McGhee RB, Freedy RM, McCalla MS. Infections of the musculoskeletal system: high-field-strength MR imaging. Radiology. 1987;164(2):449–54.
6. Levine SE, Neagle CE, Esterhai JL, Wright DG, Dalinka MK. Magnetic resonance imaging for the diagnosis of osteomyelitis in the diabetic patient with a foot ulcer. Foot Ankle Int. 1994;15(3):151–6.
7. Johnson PW, Collins MS, Wenger DE. Diagnostic utility of T1-weighted MRI characteristics in evaluation of osteomyelitis of the foot. AJR Am J Roentgenol. 2009;192(1):96–100.
8. Collins MS, Schaar MM, Wenger DE, Mandrekar JN. T1-weighted MRI characteristics of pedal osteomyelitis. AJR Am J Roentgenol. 2005;185(2):386–93.
9. Jowett AJ, Middleton SW, Quaye MC, Chesterfield H, Lasrado I, Witham FM. Intracortical haematogenous osteomyelitis. Ann R Coll Surg Engl. 2014;96(2):e13-16.
10. Prodinger PM, Pilge H, Banke IJ, Burklein D, Gradinger R, Miethke T, et al. Acute osteomyelitis of the humerus mimicking malignancy: Streptococcus pneumoniae as exceptional pathogen in an immunocompetent adult. BMC Infect Dis. 2013;13:266.
11. Zalavras CG, Rigopoulos N, Lee J, Learch T, Patzakis MJ. Magnetic resonance imaging findings in hematogenous osteomyelitis of the hip in adults. Clin Orthop Relat Res. 2009;467(7):1688–92.
12. Howe BM, Wenger DE, Mandrekar J, Collins MS. T1-weighted MRI imaging features of pathologically proven non-pedal osteomyelitis. Acad Radiol. 2013;20(1):108–14.
13. Jaramillo D, Dormans JP, Delgado J, Laor T, St Geme JW, 3rd. Hematogenous osteomyelitis in infants and children: imaging of a changing disease. Radiology. 2017; 283(3):629-643.
14. Whyte NS, Bielski RJ. Acute hematogenous osteomyelitis in children. Pediatr Ann. 2016;45(6):e204-208.
15. Trueta J. The three types of acute haematogenous osteomyelitis. J Bone Joint Surg. 1959;41B(4):671–9.
16. Kiaer T. Bone perfusion and oxygenation Animal experiments and clinical observations. Acta Orthop Scand Suppl. 1994;257:1–41.
17. Kavanagh N, Ryan EJ, Widaa A, Sexton G, Fennell J, O'Rourke S, et al. Staphylococcal osteomyelitis: disease progression, treatment challenges, and future directions. Clin Microbiol Rev. 2018;31(2):e00084-17.
18. Cook GE, Markel DC, Ren W, Webb LX, McKee MD, Schemitsch EH. Infection in Orthopaedics. J Orthop Trauma. 2015;29(Suppl 12):S19-23.
19. Carek PJ, Dickerson LM, Sack JL. Diagnosis and management of osteomyelitis. Am Fam Physician. 2001;63(12):2413–20.
20 Markanday A. Acute phase reactants in infections: evidence-based review and a guide for clinicians. Open Forum Infect Dis. 2015;2(3):ofv098.
21. Lavery LA, Ahn J, Ryan EC, Bhavan K, Oz OK, La Fontaine J, et al. What are the optimal cutoff values for ESR and CRP to diagnose osteomyelitis in patients with diabetes-related foot infections? Clin Orthop Relat Res. 2019;477(7):1594–602.
22. Wu JS, Gorbachova T, Morrison WB, Haims AH. Imaging-guided bone biopsy for osteomyelitis: are there factors associated with positive or negative cultures? AJR Am J Roentgenol. 2007;188(6):1529–34.
23. Wong A, Grando H, Fliszar E, Pathria M, Chang EY, Resnick D. Intramedullary fat globules related to bone trauma: a new MR imaging finding. Skeletal Radiol. 2014;43(12):1713–9.
24. Grey AC, Davies AM, Mangham DC, Grimer RJ, Ritchie DA. The "penumbra sign" on T1-weighted MR imaging in subacute osteomyelitis: frequency, cause and significance. Clin Radiol. 1998;53(8):587–92.
25. Gwet KL. Computing inter-rater reliability and its variance in the presence of high agreement. Br J Math Stat Psychol. 2008;61(Pt 1):29–48.
26. Calhoun JH, Manring MM. Adult osteomyelitis. Infect Dis Clin North Am. 2005;19(4):765–86.
27. Lazzarini L, Mader JT, Calhoun JH. Osteomyelitis in long bones. J Bone Joint Surg Am. 2004;86(10):2305–18.
28. Hatzenbuehler J, Pulling TJ. Diagnosis and management of osteomyelitis. Am Fam Physician. 2011;84(9):1027–33.
29. Rosenberg A, Khurana J. Osteomyelitis and osteonecrosis. Diagn Histopathol. 2016;22(10):355–68.
30. Tomlinson RE, Silva MJ. Skeletal Blood Flow in Bone Repair and Maintenance. Bone Res. 2013;1(4):311–22.
31. Colman MW, Hornicek FJ, Schwab JH. Spinal cord blood supply and its surgical implications. J Am Acad Orthop Surg. 2015;23(10):581–91.
32. Palestro CJ, Love C, Miller TT. Infection and musculoskeletal conditions: Imaging of musculoskeletal infections. Best Pract Res Clin Rheumatol. 2006;20(6):1197–218.
33. Mader JT, Mohan D, Calhoun J. A practical guide to the diagnosis and management of bone and joint infections. Drugs. 1997;54(2):253–64.
34. Calhoun JH, Manring MM, Shirtliff M. Osteomyelitis of the long bones. Semin Plast Surg. 2009;23(2):59–72.
35. Garcia Del Pozo E, Collazos J, Carton JA, Camporro D, Asensi V. Bacterial osteomyelitis: microbiological, clinical, therapeutic, and evolutive characteristics of 344 episodes. Rev Esp Quimioter. 2018;31(3):217–25.
36. Barakat E, Guischer N, Houssiau F, Lecouvet FE. The "birth of death": MRI step-by-step reveals the early appearance of a bone marrow infarct. Acta Radiol Open. 2019;8(3):2058460119834691.
37. Murphey MD, Foreman KL, Klassen-Fischer MK, Fox MG, Chung EM, Kransdorf MJ. From the radiologic pathology archives imaging of osteonecrosis: radiologic-pathologic correlation. Radiographics. 2014;34(4):1003–28.
38. Blacksin MF, Finzel KC, Benevenia J. Osteomyelitis originating in and around bone infarcts: giant sequestrum phenomena. AJR Am J Roentgenol. 2001;176(2):387–91.